JCS ePress online publication date 19 January 2010

Membrane protein SMP-1 is required for normal flagellum function in *Leishmania*

Dedreia Tull[1,*], Thomas Naderer[1,*], Timothy Spurck[2], Haydyn D. T. Mertens[1], Joanne Heng[1], Geoffrey I. McFadden[2], Paul R. Gooley[1,‡] and Malcolm J. McConville[1,‡,§]

[1]Department of Biochemistry and Molecular Biology, Bio21 Molecular Science and Biotechnology Institute and [2]School of Botany, University of Melbourne, Parkville, Victoria, Australia

*These authors contributed equally to this work
‡These authors contributed equally to this work
§Author for correspondence (malcolmm@unimelb.edu.au)

Accepted 28 October 2009
Journal of Cell Science 123, 544-554 Published by The Company of Biologists 2010
doi:10.1242/jcs.059097

Summary

Eukaryotic flagella and cilia are surrounded by a membrane that is continuous with, but distinct from, the rest of the plasma membrane. In *Leishmania* parasites, the inner leaflet of the flagellar membrane is coated with the acylated membrane protein, SMP-1. Here, we provide evidence that SMP-1 stabilizes the flagellar membrane and is required for flagella elongation and function. The expression and flagella targeting of SMP-1 is tightly associated with flagella elongation during amastigote to promastigote differentiation. Deletion of the genes encoding SMP-1 and the flagellar pocket protein SMP-2, led to the production of short flagella and defects in motility. Alterations in the physical properties of the *smp-1/smp-2*$^{-/-}$ flagellar membrane were suggested by: (1) the accumulation of membrane vesicles in the flagellar matrix, and (2) further retraction of flagella following partial inhibition of sterol and sphingolipid biosynthesis. The flagella phenotype of the *smp-1/smp-2*$^{-/-}$ null mutant was reversed by re-expression of SMP-1, but not SMP-2. SMP-1 contains a jelly-roll β-sheet structure that is probably conserved in all SMP proteins, and forms stable homo-oligomers in vivo. We propose that the SMP-1 coat generates and/or stabilizes sterol- and sphingolipid-rich domains in the flagellar membrane.

Key words: Flagellum membrane, Myristylated protein, Jelly-roll β-sheet, Lipid rafts

Introduction

Eukaryotic flagella and cilia are highly conserved organelles that project from the surface of many cells and are involved in cell motility and/or solute movement over the cell surface. They can also contain protein receptors, signaling proteins and nutrient channels involved in chemosensory, mechanosensory and photosensory behaviour (Scholey and Anderson, 2006). These structures minimally comprise an internal microtubule-based axoneme and a specialized membrane that has a distinct protein and lipid composition from other plasma membrane domains (Vieira et al., 2006). Flagellar assembly and maintenance are highly dynamic processes that are dependent on the import and recycling of axonemal, matrix and membrane proteins. Although the processes that underlie the import of flagellar axonemal and matrix proteins have been intensively studied (Rosenbaum and Witman, 2002), much less is known about mechanisms that target membrane proteins to these structures, and the role of membrane proteins in flagellar biogenesis. Unlike axonemal and matrix proteins that are synthesized in the cytosol and transported to flagella by intraflagellar transport (IFT) protein complexes, flagellar membrane proteins are synthesized in the ER and transported to the plasma and flagellar membrane via the Golgi complex. Vesicle transport to the flagellum appears to be regulated by a number of specific effector proteins (Rab8, Arl-3), cargo adaptors (AP-μ1 subunit, STAM) (Bae et al., 2006; Dwyer et al., 2001; Hu et al., 2007), phosphoinositides (Wei et al., 2008) and non-IFT cytoplasmic protein complexes (Bardet-Biedi syndrome, OSEG and exocyst proteins) (Avidor-Reiss et al., 2004; Cuvillier et al., 2000; Dwyer et al., 2001; Hu et al., 2007; Nachury et al., 2007; Pullen et al., 2004; Qin et al., 2005; Rosenbaum and Witman, 2002; Sahin et al., 2008a; Scholey and Anderson, 2006; Wei et al., 2008; Zuo et al., 2009). Although it is generally assumed that the axoneme provides the structural template for the flagellar membrane, the extent to which flagellar membrane dynamics regulate axoneme biogenesis and maintenance is not understood.

The trypanosomatidae are a group of flagellated protozoa that cause a number of important diseases in humans, including human African trypanosomiasis (*Trypanosoma brucei*), Chagas disease (*Trypanosoma cruzi*) and the leishmaniases (*Leishmania* spp.). Motile stages of these parasites produce a single flagellum that emerges from a specialized invagination in the plasma membrane, termed the flagellar pocket. The emergent flagellum contains a typical 9+2 microtubule axoneme that is supported by a paracrystalline structure called the paraflagellar rod (PFR) (Ginger et al., 2008; Ralston and Hill, 2008). The trypanosomatid flagellum and associated flagellar pocket is required for motility, endocytosis and exocytosis, and cytokinesis (Bonhivers et al., 2008; Broadhead et al., 2006; Ginger et al., 2008; Kohl et al., 2003; McConville et al., 2002; Ralston and Hill, 2008). Specific nutrient transporters and signaling proteins are also targeted to the flagellar membrane, indicating a role for the flagellum in environmental sensing (Ginger et al., 2008; Oberholzer et al., 2007). Recent studies have confirmed that IFT has a central role in regulating the assembly and maintenance of the axonemal and paraflagellar rod structures in trypanosomatids, as in other eukaryotes (Absalon et al., 2008; Davidge et al., 2006; Ginger et al., 2008). A number of proteins involved in membrane transport have also been shown to have a role in regulating flagellum assembly. Specifically, overexpression of a constitutively active form of *Leishmania donovani* Arl-3, or targeted deletion of the *Leishmania mexicana* adaptor protein-1 σ-

subunit, induced a dramatic shortening of the flagellum in promastigotes stages (Cuvillier et al., 2000; Vince et al., 2008). Similarly, pharmacological or genetic inhibition of sterol or sphingolipid biosynthesis results in defects in flagellum biogenesis (Denny et al., 2004; Tull et al., 2004; Zhang et al., 2003). The latter studies suggest that processes involved in defining the properties of the flagellar membrane are likely to be crucial for flagellar biogenesis and function.

In this study, we investigated the function of an abundant *Leishmania* flagellar membrane protein, termed the small myristoylated protein-1 (SMP-1). SMP-1 is a 15 kDa protein, initially identified in a proteomic analysis of *L. major* detergent-resistant membranes (DRMs) and is both N-myristoylated and S-palmitoylated in vivo (Tull et al., 2004). SMP-1 is exclusively localized to the flagellum and, based on estimated copy number (10^5 copies/cell), is likely to coat the inner leaflet of the flagellar membrane (Tull et al., 2004). SMP-1 can be readily extracted from flagellar membranes under conditions that solubilize DRMs, but not flagellar axonemal components, indicating the absence of strong association between the membrane-bound SMP-1 and the axoneme. Interestingly, the *Leishmania* genome encodes a number of other proteins that share close sequence homology to SMP-1. Moreover, SMP-1-like domains have been identified at the N-termini of a large family of calpain-like proteins and are likely to be responsible for targeting these proteins to the cytoplasmic leaflet of endo- and plasma membranes (Ersfeld et al., 2005; Hertz-Fowler et al., 2001). Currently, little is known about the function of any of these proteins. In this study, we determined the structure of SMP-1 and provide evidence that it is required for normal flagellum function, in part by stabilizing the DRM-rich flagellar membrane.

Results

SPM-1 is an early marker of flagellum elongation

We have previously shown that SMP-1 is expressed at high levels in promastigotes stages and is distributed along the length of the flagellum that extends beyond the opening of the flagellar pocket (Tull et al., 2004). By contrast, SMP-1 is not detected in non-motile amastigotes stages, which contain a short flagellum that is completely contained within the flagellar pocket (Tull et al., 2004). To establish whether SMP-1 expression is linked to flagellum elongation, SMP-1 expression was monitored at various time points during amastigote to promastigote differentiation. Differentiation occurs over ~40 hours and is associated with the elongation of the cell body and emergence of an unattached flagellum from the flagellar pocket. SMP-1 expression was detected before the flagellum began to extend beyond the flagellar pocket, after 24 hours (Fig. 1A), and preceded that of the paraflagellar rod protein 1 (PFR-1), which forms part of the major accessory cytoskeletal structure in emergent sections of the flagellum (Fig. 1B). SMP-1 was initially concentrated at the distal end of the new flagellum, but became evenly distributed along the entire length of the elongated flagellum in fully differentiated promastigotes. These data show

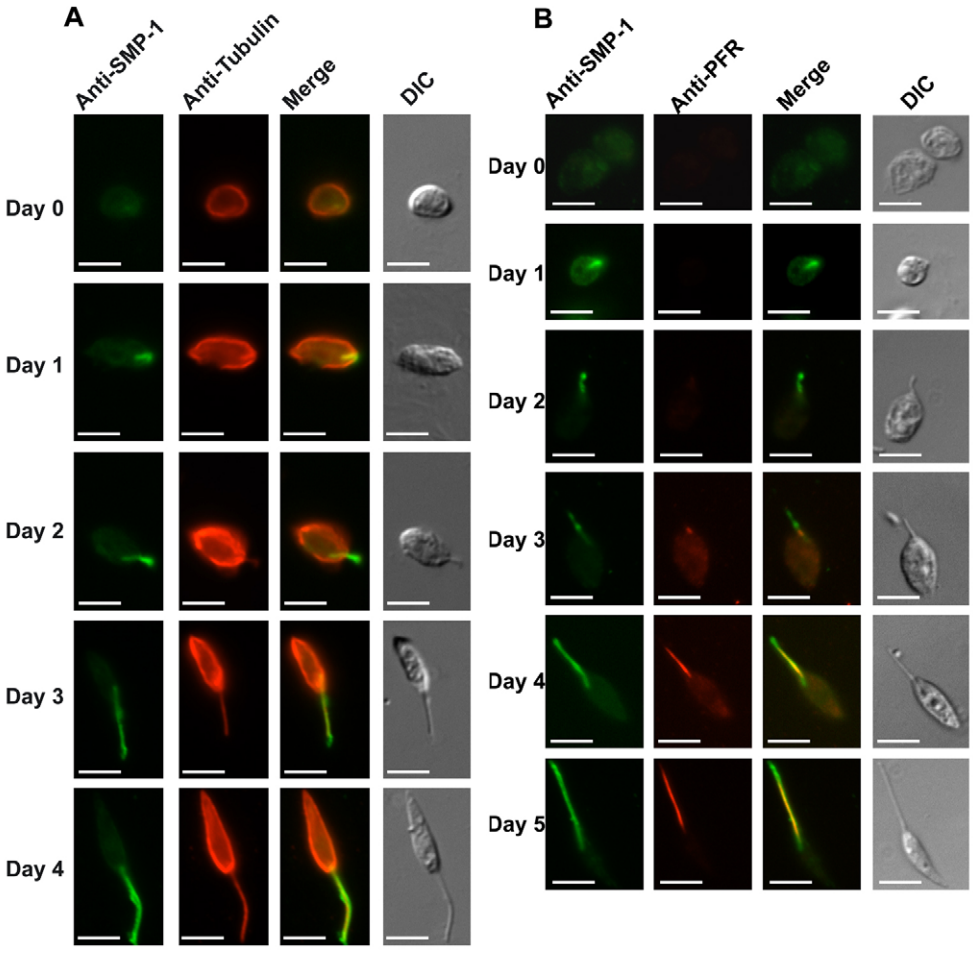

Fig. 1. SMP-1 expression precedes the formation of an emergent flagellum during amastigote to promastigote differentiation. Lesion-derived amastigotes were suspended in SDM medium, pH 7.5, and cultured at 27°C for 5 days. Aliquots of differentiating parasites were fixed at 24 hour intervals and probed (**A**) with antibodies against SMP-1 (green signal) and tubulin (red signal) or (**B**) with antibodies against SMP-1 (green signal) and PFR (L8C4; red signal). Scale bars: 5 μm.

that SMP-1 is one of the first specific markers of flagellum elongation during amastigote to promastigote differentiation.

SMP-1 and SMP-2 have distinct subcellular localizations

Genes encoding SMP-1 and the closely related protein, SMP-2, are tandemly linked with each other on chromosome 20 (Tull et al., 2004). To determine whether SMP-2 might be functionally related to SMP-1, HA-epitope tagged versions of SMP-1 and SMP-2 were expressed in wild type *L. major* promastigotes and their localization determined by fluorescence microscopy. Both proteins were metabolically labeled with [^{3}H]myristic acid, indicating that they are acylated in vivo (data not shown). Although SMP-1::HA localized to the flagellar membrane (supplementary material Fig. S1), SMP-2::HA was targeted to a single, punctate structure at the apical end of the parasite (Fig. 2A). SMP-2::HA staining was always tightly associated with the proximal end of the flagellum and juxtaposed to the kinetoplast, a structure in the anterior lobe of the mitochondria that is physically tethered to the basal body of the flagellum (Fig. 2A). These observations suggested that SMP-2 is localized to either the flagellar pocket membrane or the flagellar basal body. To distinguish between these possibilities, *L. major* promastigotes expressing the SMP-2::HA were solubilized in 1% Triton X-100 at either 4°C or 25°C. Acylated proteins, such as SMP-1, are solubilized by 1% Triton X-100 at 25°C but are resistant to extraction at 4°C (Fig. 2B), indicating an association with DRMs (Ralton et al., 2002; Tull et al., 2004). However, the flagellar axoneme and PFR are insoluble in 1% Triton X-100 at both 4°C and 25°C (Tull et al., 2004). By contrast, SMP-2::HA (and endogenous SMP-2; data not shown) was solubilized in 1% Triton X-100 at both 4°C (Fig. 2B) and 25°C (data not shown). These data suggest that SMP-2::HA is targeted to the flagellar pocket membrane and that this membrane is more readily detergent solubilized than either the cell body or flagellar membrane. Interestingly, overexpression of SMP-2::HA resulted in additional targeting to the cell body plasma membrane (supplementary material Fig. S1), suggesting that this is the default localization when flagellar-pocket targeting or retention mechanisms are saturated. However, SMP-2::HA fluorescence was never observed in the flagellum, supporting the conclusion that SMP-2 is functionally distinct from SMP-1.

Analysis of a *L. major* mutant lacking SMP-1 and SMP-2

A *L. major* mutant lacking both SMP-1 and SMP-2 was generated to further investigate the function of these proteins. The two chromosomal loci containing the genes encoding SMP-1 and SMP-2 were replaced with antibiotic cassettes conferring resistance to bleomycin and puromycin. Western blot analysis of the heterozygous (*L. major smp-1/smp-2*$^{-/+}$) and homozygous (*L. major smp-1/smp-2*$^{-/-}$) null mutants showed that SMP-1 and SMP-2 levels were reduced or absent, respectively (Fig. 3A). The *L. major smp-*

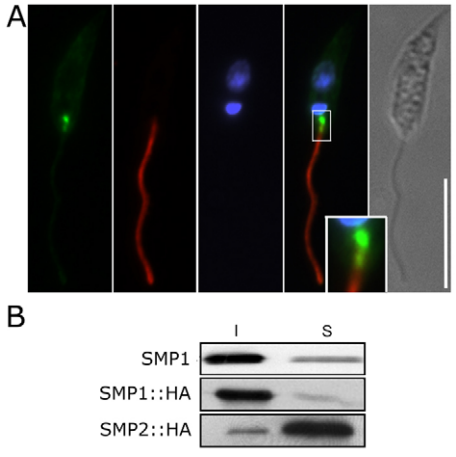

Fig. 2. Localization of *L. major* SMP family proteins. (**A**) *L. major* promastigotes expressing SMP-2::HA were labeled with anti-SMP-1 (red signal), anti-HA (green signal) and Hoechst dye (nucleus and kinetoplast, blue signal) after fixation. Scale bar: 10 µm. (**B**) *L. major* promastigotes expressing either SMP-1::HA or SMP-2::HA were extracted in 1% Triton X-100 at 4°C and proteins in the soluble and insoluble fractions analysed by SDS-PAGE and western blotting. SMP-1 and SMP-2::HA were detected with antibodies against SMP1 and the HA epitope, respectively.

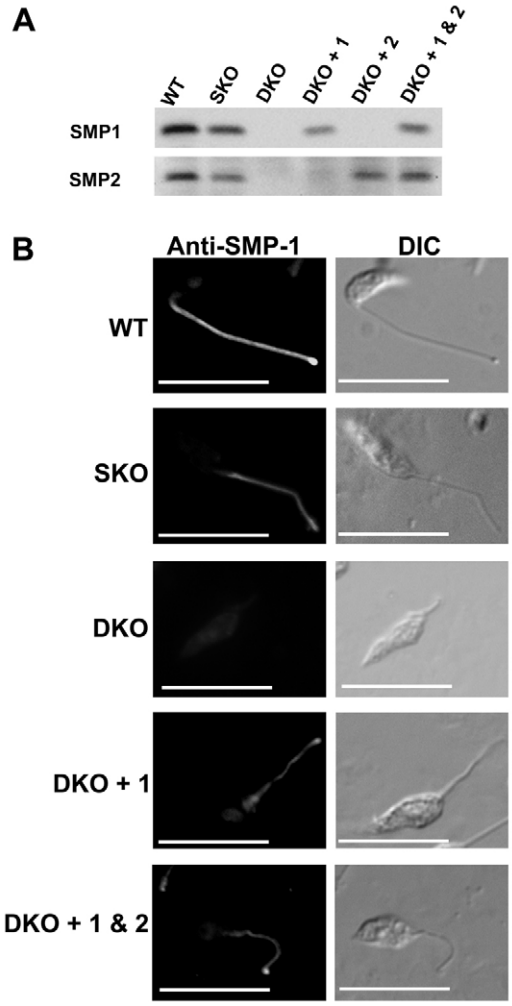

Fig. 3. Generation of *L. major smp-1/smp-2*$^{-/-}$ mutant. (**A**) Total protein was extracted from *L. major* wild type (WT), *smp-1/smp-2*$^{-/+}$ (SKO), *smp-1/smp-2*$^{-/-}$ (DKO), *smp-1/smp-2*$^{-/-}$::SMP-1 (DKO+1), *smp-1/smp-2*$^{-/-}$::SMP-2 (DKO+2) and *smp-1/smp-2*$^{-/-}$::SMP1::SMP2 (DKO+1 & 2) were analysed by SDS-PAGE and SMP proteins detected using anti-SMP-1 and anti-SMP-2 antibodies. The same cell equivalents were loaded for each cell line. (**B**) Wild-type, SKO, DKO and complemented DKO promastigotes were fixed and probed with anti-SMP-1 antibody and analysed by indirect immunofluorescence microscopy. Scale bars: 10 µm.

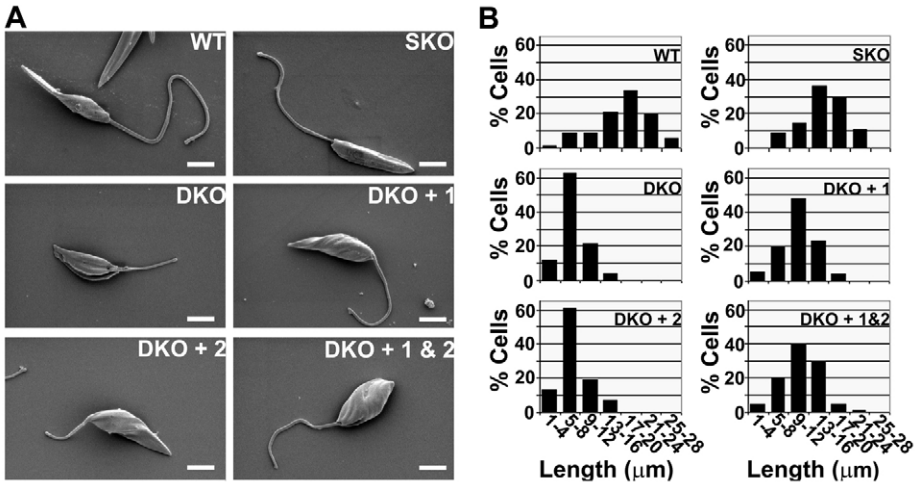

Fig. 4. Deletion of SMP-1 causes shortening of the flagellum. (**A**) Wild-type (WT), *smp-1/smp-2*$^{-/+}$ (SKO), *smp-1/smp-2*$^{-/-}$ (DKO) and DKO complemented parasite lines were fixed and analysed by scanning electron microscopy. (**B**) Flagellum length distributions measured using Image I software. Scale bars: 2 μm.

1/smp-2$^{-/-}$ null mutant was complemented with plasmids encoding SMP-1 or SMP-2 or both SMP-1 and SMP-2. SMP-1 and SMP-2 were detected in the relevant add-back parasite lines, although levels of expression of SMP-1 were always less than in the wild-type parasites (Fig. 3A), reflecting the high levels of endogenous expression of SMP-1. Ectopically expressed SMP-1 (Fig. 3B) and SMP-2 (data not shown) were correctly targeted to the flagellum and flagellar pocket of the *L. major smp-1/smp-2*$^{-/-}$ mutant, respectively.

The *smp-1/smp-2*$^{-/-}$ mutant had the same growth characteristics as wild-type parasites in rich culture medium (data not shown). However, initial light and fluorescence microscopy analyses indicated that *smp-1/smp-2*$^{-/-}$ promastigotes had shorter flagella than wild-type parasites. This phenotype was quantified by scanning electron microscopy of the flagella in the wild-type, mutant and complemented parasite lines (Fig. 4A). The flagella of wild-type parasites had an average length of 17±5 μm (Fig. 4B). Flagella length was slightly reduced in the heterozygote knockout mutant (15±4 μm), and very significantly reduced in the null mutant (6±3 μm) (Fig. 4B). More than 90% of the wild type, but fewer than 20% of mutant parasites had flagella that were longer than 8 μm. Interestingly, the cell body of the null mutants (9±2 μm) was also shorter than those of the wild type (15±2 μm) (Fig. 4A). Ectopic expression of SMP-2 in the *smp-1/smp-2*$^{-/-}$ mutant did not restore the wild-type flagellar phenotype. By contrast, ectopic expression of SMP-1 (either by itself, or together with SMP-2) resulted in an approximate doubling of the length of the flagellum in the mutant (average length 11±3 μm). The incomplete restoration of flagella length probably reflects the lower levels of expression of SMP-1 in the complemented strains compared with wild-type parasites (Fig. 3A). These analyses show that wild-type levels of SMP-1 expression are required to maintain normal flagellum length.

Loss of SMP-1 results in a defect in cell motility

Investigation of the wild-type, *smp-1/smp-2*$^{-/-}$ mutant and complemented strains by video microscopy indicated that the shortened flagellar phenotype had a dramatic effect on promastigote motility (Fig. 5; supplementary material Movies 1 and 2). The flagella of wild-type and *smp-1/smp-2*$^{+/-}$ heterozygote parasites exhibited a regular sigmoidal beat and more than 90% of these parasites were motile and capable of swimming extended distances in one direction. The average speed of wild-type parasites was 16 μm/second, although some cells could swim as fast as 26-30 μm/second. Although the rate profile of the single allele deletion mutant was slightly reduced compared with that in wild-type parasites (12 μm/second), the *smp-1/smp-2*$^{-/-}$ promastigotes were either

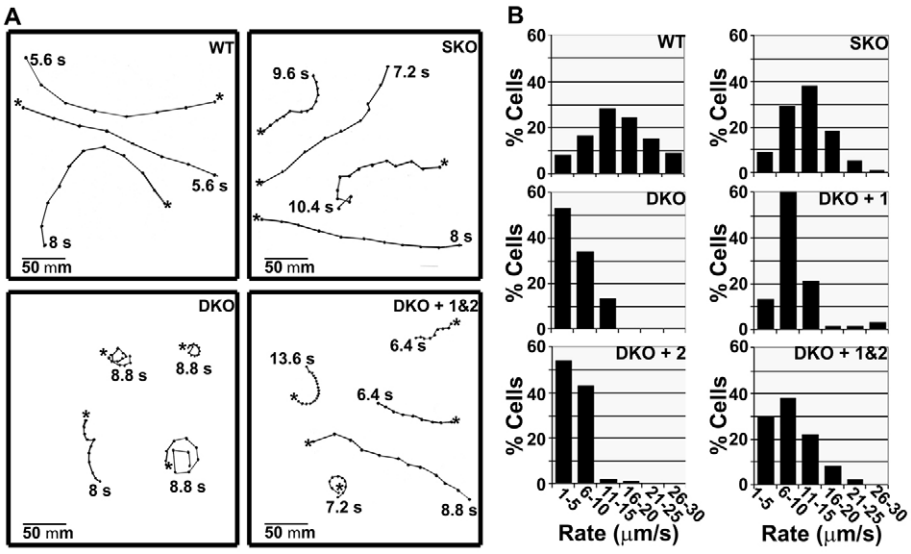

Fig. 5. Deletion of SMP-1 impairs directional motility. Wild type (WT), *smp-1/smp-2*$^{-/+}$ (SKO), *smp-1/smp-2*$^{-/-}$ (DKO) and DKO complemented parasite lines (DKO + 1&2) were analysed by video microscopy and the data used to generate (**A**) motility traces and (**B**) motility rates.

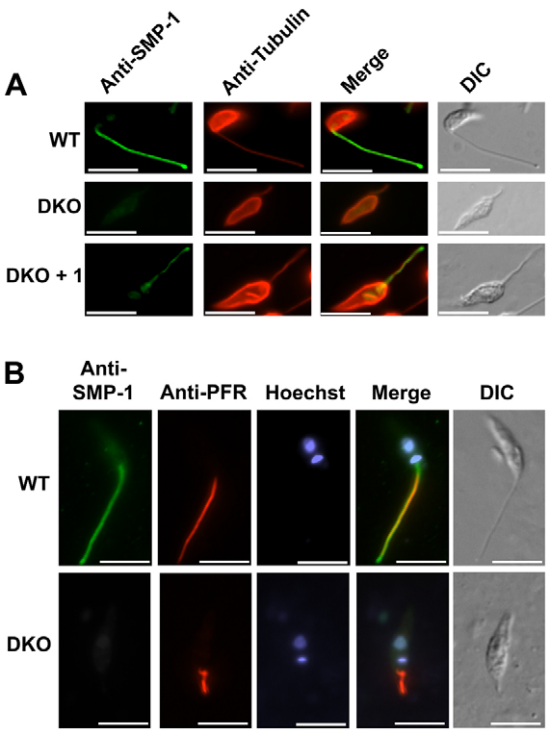

Fig. 6. The short flagella of *smp-1/2*$^{-/-}$ parasites retain an axoneme and paraflagellar rod. Wild-type (WT), *smp-1/smp-2*$^{-/-}$ (DKO) and *smp-1/smp-2*$^{-/-}$::*SMP-1* (DKO+1) promastigotes were fixed and probed with (**A**) antibodies to SMP-1 (green) and tubulin (red) or (**B**) antibodies to SMP-1 (green) and anti-PFR (red) antibodies and analysed by indirect immunofluorescence microscopy. Scale bars: 10 µm.

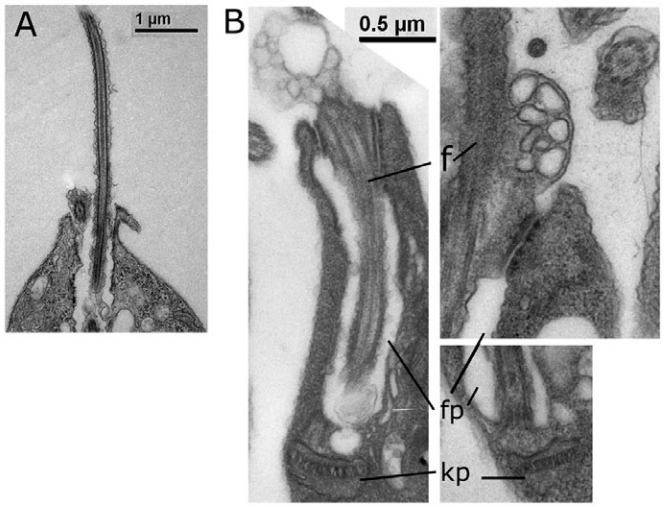

Fig. 7. Ultrastructural changes in the flagellar membrane of *smp-1/smp-2*$^{-/-}$ parasites. *L. major* wild-type and *smp-1/smp-2*$^{-/-}$ promastigotes were fixed in glutaraldehyde and osmium tetraoxide and serial sections (90 nm) examined by TEM. Representative sections of (**A**) wild-type *L. major* promastigotes and (**B**) *smp-1/smp-2*$^{-/-}$ promastigotes. The latter accumulate membrane vesicles in the flagellar matrix, which are absent in the flagella of wild-type parasites (A). f, flagellum; fp, flagellum pocket; kp, kinetoplast.

immobile, or exhibited uncontrolled movement and/or swam in circles (Fig. 5). The immobile *smp-1/smp-2*$^{-/-}$ promastigotes generally exhibited flagella that were less than 50% of the length of wild-type parasites, whereas those with uncontrolled movements had somewhat longer flagella (>50% of the length of the flagellum of wild-type parasites). The latter parasites also swam more slowly than wild-type parasites, typically at rates ≤5 µm/second. Ectopic expression of SMP-2 in the mutant parasites did not restore directional motility in this subpopulation of mutant parasites. By contrast, ectopic expression of SMP-1 in the null mutant or the null mutant co-expressing SMP-1 and SMP-1, restored directional motility, as well as swim speeds. These analyses confirm that SMP-1 is required for normal flagellar function.

Loss of SMP-1 results in aberrant flagellar membrane structure

To further define the nature of the defect in flagellar biogenesis in the *smp-1/smp-2*$^{-/-}$ mutant, the structure of the flagellum in wild-type and mutant parasites was examined in more detail. The flagella of mutant parasites contained a microtubule axoneme and paraflagellar rod, as shown by both indirect immunofluorescence and transmission electron microscopy (Figs 6,7). As in wild-type parasites, the paraflagellar rod of mutant parasites extended from near the flagellar base (where the flagellum emerges from the flagellar pocket) to the distal tip of the flagellum (Fig. 6). These analyses also revealed major changes in membrane dynamics within the flagella. Specifically, the flagella of *smp-1/smp-2*$^{-/-}$ mutants contained numerous membrane vesicles, 25-240 nm in diameter, that accumulated in the flagellar matrix space between the axoneme and the limiting membrane (Fig. 7B). These vesicles were shown by serial sectioning to be separate from each other and from the limiting membrane. Similar membrane structures were absent from the flagellum of wild-type parasites processed in parallel, indicating that these structures were not an artifact of the fixation conditions (Fig. 7A). Significantly, increased membrane vesicle formation was not observed in the cytosol of the mutant. Nor were membrane vesicles ever seen in the lower sections of the flagella contained within the flagellar pocket (Fig. 7B). These data suggest that the intraflagella membrane vesicles are not derived from cytosolic vesicles, but probably result from involution of the flagellar membrane.

SMP-1 stabilizes the flagellar membrane from perturbation in lipid composition

The changes in flagellar membrane ultrastructure in *smp-1/smp-2*$^{-/-}$ parasites suggested that SMP-1 stabilizes this membrane. To test whether SMP-1 protects the flagellum from perturbation in lipid composition, wild-type and *smp-1/smp-2*$^{-/-}$ parasites were treated with sublethal concentrations of ketoconazole and myriocin. Ketoconazole inhibits the enzyme, sterol 14′-demethylase, leading to the accumulation of ergosterol precursors, whereas myriocin inhibits serine:palmitoyl-CoA sphingosine synthase, resulting in depletion of de novo synthesized sphingolipids (Tull et al., 2004). Ketoconazole treatment (0.5 µg/ml, 48 hours) of wild-type parasites had little effect on flagellar length (Fig. 8) (Tull et al., 2004). By contrast, ketoconazole treatment caused the flagella of *smp-1/smp-2*$^{-/-}$ parasites to retract by >80% after 48 hours of treatment (Fig. 8). Similarly, inhibition of sphingolipid biosynthesis with myriocin had no effect on flagellar length in wild-type parasites, but induced pronounced flagellar retraction in the mutant (Fig. 8). Ectopic expression of SMP-1::HA in the *smp-1/smp-2*$^{-/-}$ mutant largely reversed the effects of ketoconazole and myriocin on flagellar

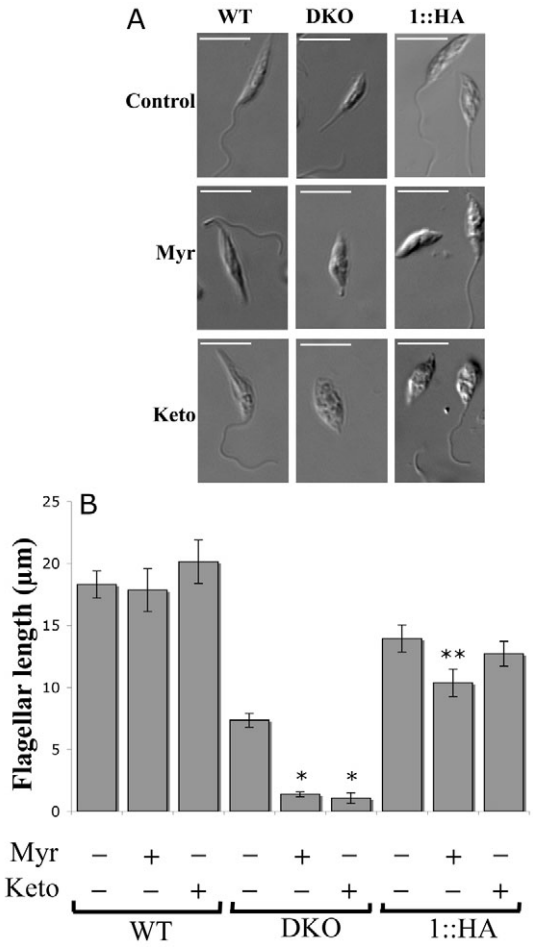

Fig. 8. Deletion of SMP-1 leads to increase susceptibility of the flagellum to inhibitors of sterol and sphingolipid biosynthesis. Wild-type (WT), *smp-1/smp-2*$^{-/-}$ (DKO) and *smp-1/smp-2*$^{-/-}$ parasites expressing HA-tagged SMP-1 (1::HA) were treated of ketoconazole (Keto, 0.5 μg/ml) or myriocin (Myr, 1 μg/ml) for 48 hours. Promastigotes were fixed and analysed by DIC microscopy (**A**) and flagellar length was quantified (**B**). Error bars represent s.e.m. *P* values were derived from drug-treated compared with untreated cells using the Student's *t*-test (unpaired, two-tailed), **P*<0.001 and ***P*<0.05.

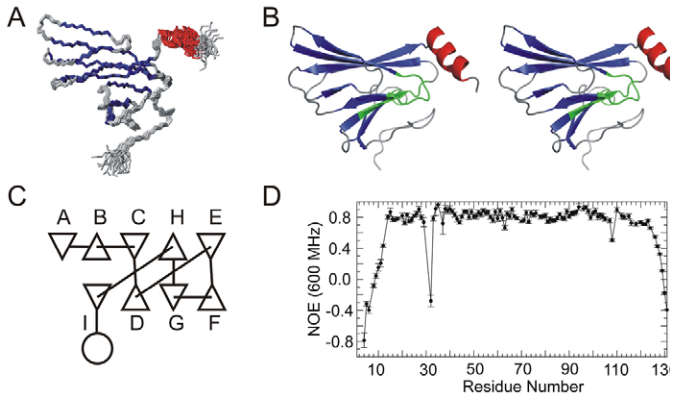

Fig. 9. NMR solution structure of SMP-1. (**A**) Family of the 24 best structures of SMP-1 superimposed on residues 12-120. The disordered region encompassing residues 1-7 is excluded for clarity. Highlighted in green are the residues of the three motifs that are conserved in all SMP/SKCRP/CALP domain I sequences. In SMP-1 these correspond to residues 35-38 (GLLF/Y), residues 48-54 (WFFYNDT) and residues 93-98 (VVPxETE) (Tull et al., 2004). (**B**) Ribbon stereodiagram of a representative structure. (**C**) Topology diagram showing the characteristic β-sandwich 'jelly-roll' fold of SMP-1. (**D**) Heteronulcear $^{1}H\{^{15}N\}$-NOE data for SMP-1 acquired at 25°C and pH 6.8.

morphology (Fig. 8). These experiments show that expression of SMP-1 attenuates the effects of membrane-perturbing agents on flagellar structure.

Structure of SMP-1 and organization in the flagellar membrane

To gain further insight into the role of SMP-1, the solution structure of non-acylated SMP-1 was determined by NMR (Fig. 9; supplementary material Table S1). Non-acylated SMP-1 is a monomer in solution and contains a classic β-sandwich jelly-roll topology, with two anti-parallel β-sheets (β-sheet 1: β1, β2, β3, β8, β5 and β-sheet 2: β9, β4, β7, β6, respectively) (Williams and Westhead, 2002). All strands were regular except for a distinct β-bulge in the centre of β8 that breaks the contact with the short outer β5 strand. Sequence motifs that are conserved in all SMP/CALP domain I proteins were highly concentrated around one end of the inner β-sheet 1 and connecting loops (coloured green, Fig. 9B). The N-terminus of non-acylated SMP-1 contained a short, unstructured sequence (residues 1-12) that is likely to be solvent exposed (corresponding to the site of myristoylation and palmitoylation), a prominent loop structure (residues 14-19) and an extended strand that runs underneath and perpendicular to β-sheet 1 (residues 20-24). No obvious main chain hydrogen bond patterns stabilized this N-terminal region, but the side chains of residues 14-24 clearly packed with those of the inner β-sheet to form a distinct hydrophobic core [Tyr14 and Pro19, Val26 (β1), Phe38 and Ile40 (β2), and Tyr51 (β3)]. The unique C-terminus of SMP-1 comprised an α-helix (residues 120-129) that sits on top of β-sheet 2 running across the top and perpendicular to this sheet (Fig. 9). The α-helix is distinctly hydrophilic and is partially stabilized in the first two turns by an aromatic cluster between Tyr122 and His125 of the helix and Tyr94 of the β-sheet. Heteronuclear $^{1}H\{^{15}N\}$-nuclear Overhauser effect (NOE) analyses indicated that the loops around residues 30 and 108 were relatively flexible (NOE values of less than 0.6) (Fig. 9D). These regions contained peaks that were either very weak or absent, indicating motion on an intermediate timescale. Very low NOE values ($\ll$0.6) were observed for the N- (first 12 residues) and C-termini (last seven residues) indicative of marked dynamic disorder on the nanosecond timescale. These analyses suggest that the acylated N-terminal domain is normally solvent exposed, possibly facilitating the insertion of N-terminal myristoyl or palmitoyl groups into the target membrane. However, the unique C-terminal helix of SMP-1 was orientated perpendicular to the outer β-sheet 2 and away from the membrane. Replacement of the C-terminal helix with other sequences, as occurs in other SMP proteins and in the large calpain superfamily, would not be expected to alter the conserved β-sheet core structure of these proteins. The SMP-1 module can thus be viewed as a versatile membrane adaptor for a wide range of peptide and polypeptide sequences.

Comparative structural analysis using the DALI search engine confirmed that SMP-1 had a similar structure to other protein domains containing the β-sandwich jelly-roll fold. Highest DALI

scores (15.9) were observed for another hypothetical *Leishmania* protein (LmjF20.1230, pdb lr75) (Arakaki et al., 2003), which has recently been classified as a myristoylated member of the CALP/SMP protein family, LmSKCP20.6 (Ersfeld et al., 2005). Overlay of the NMR and crystal structures of SMP-1 and SKCP20.6, respectively, revealed a remarkable degree of structural conservation between these two proteins (supplementary material Fig. S2), indicating that this fold has been retained in all SMP/SKCP family members. The next most closely related folds were found in a number of viral coat proteins (e.g. the carnation mottle virus coat protein, pdb ID 1opo, DALI score 4.6), bacterial toxins (e.g. diphtheria toxin, pdb ID 1f0l, DALI score 4.4), and the ectodomain of the glucocorticoid-induced TNF receptor ligand (pdb ID 3b94, DALI score 4.6). The lower DALI scores reflect weak sequence and poor structural alignment between SMP-1 and these proteins (Nandhagopal et al., 2002; Williams and Westhead, 2002).

A number of proteins with the β-sandwich jelly-roll fold self-associate in vivo to form homo-oligomers (Chattopadhyay et al., 2007; Nandhagopal et al., 2002). To investigate whether SMP-1 self-associates in vivo, wild-type and *smp-1/smp-2*$^{-/-}$ parasites were incubated with the cell-permeable cross-linking agent DSS, and complexes were analysed by SDS-PAGE and western blotting. As shown in Fig. 10B, protein bands that reacted with anti-SMP-1 antibody were detected at 15, 30 and 45 kDa in wild-type parasite extracts, but not in the *smp-1/smp-2*$^{-/-}$ mutant, which is consistent with the presence of monomers, homodimers and homotrimers in vivo. Similar results were obtained when the water-soluble cross-linking agent DTSSP was used to crosslink proteins in Triton-X-100-insoluble membranes (Fig. 10A). Again, no evidence for hetero-oligomeric complexes between SMP-1 and other proteins was detected (Fig. 10B). Finally, the presence of flagellar membrane SMP-1 oligomers was assessed after mild detergent solubilization of parasite membranes with lauryl maltoside, and analysis of resulting complexes by two-dimensional blue native (BN)-SDS-PAGE. SMP-1 associated with a very high molecular weight complex or aggregate near the top of the first dimension (Fig. 10C). This aggregate might correspond to large DRM domains (Fig. 10C). Following separation in the second dimension (SDS-PAGE with non-reducing conditions), SMP-1 monomers, dimers and trimers were detected (Fig. 10C). These data suggest that diacylated SMP-1 self-associates to form relatively stable oligomers, in the presence or absence of chemical cross-linkers, in vivo. Such interactions might stabilize the SMP-1 coat that covers the inner leaflet of the flagellar membrane.

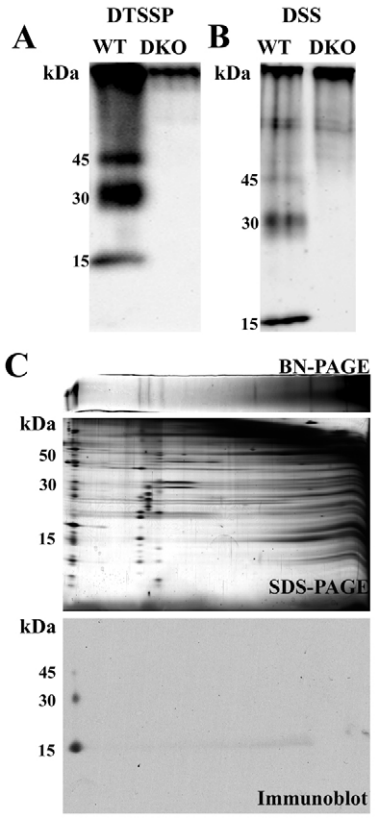

Fig. 10. SMP-1 forms homo-oligomers in vivo. (**A**) Wild-type and *smp-1/smp-2*$^{-/-}$ (DKO) parasites were extracted with cold Triton X-100 and the insoluble DRM fraction incubated with the crosslinking reagent DTSSP. Proteins were analysed by SDS-PAGE and SMP-1 detected by western blotting using anti-SMP-1 antibody. Bands corresponding to SMP-1 monomers (15 kDa), dimers (30 kDa) and trimers (45 kDa), were detected in wild-type, but not the *smp-1/smp-2*$^{-/-}$ extracts. (**B**) Wild-type and *smp-1/smp-2*$^{-/-}$ mutant parasites were incubated with the membrane-permeable crosslinking reagent DSS, and DRM proteins analysed by western blot using the anti-SMP-1 antibody. (**C**) Wild-type parasites were extracted with lauryl maltoside without chemical crosslinking and the protein complexes resolved by two-dimensional BN-PAGE. The upper panel shows high molecular mass proteins complexes resolved by BN-PAGE (the resolving gel is on the left). In the middle panel, complexes resolved in the first dimension are analysed by SDS-PAGE under non-reducing conditions. Proteins in the first and second dimensions were stained with Coomassie Blue. In the bottom panel, proteins in the two-dimensional BN-PAGE were transferred to PVDF membranes and SMP-1 detected by western blotting. SMP-1 monomers, dimers and trimers were identified in a high molecular mass complex aggregate that migrated near the top of the first dimension. Molecular size markers are indicated on left hand side of the SDS-PAGE and western blot.

Discussion

The limiting membrane of eukaryotic flagella constitutes a unique subdomain of the plasma membrane with a distinctive protein and lipid composition. Although the biogenesis of axoneme and matrix components of flagella has been intensively studied, the mechanisms involved in generating and maintaining the flagellar membrane are still poorly defined. In this study, we show that the diacylated membrane protein SMP-1 is required for normal flagellar biogenesis in *Leishmania* promastigote stages. First, SMP-1 expression was found to be tightly associated with the formation of the elongated flagellum during amastigote to promastigote differentiation. SMP-1 was detected as soon as the flagellum began to extend beyond the opening of the flagellar pocket and preceded the expression of other proteins associated with the emergent flagellum, such as the paraflagellar rod protein-1. Second, deletion of the tandemly linked genes encoding SMP-1 and SMP-2 resulted in a pronounced defect in flagellum elongation and function. Promastigote stages of the *smp-1/smp-2*$^{-/-}$ mutant had much shorter flagella than wild-type parasites, as well as defects in directional swimming. Both phenotypes were partially rescued by ectopic expression of SMP-1, but not SMP-2. It is likely that very high levels of expression of SMP-1, approaching levels observed in wild-type parasites, are needed for complete rescue of the *Δsmp-1/smp-2*$^{-/-}$ phenotype. These data are consistent with SMP-1 having a structural role within the flagella. They also show that SMP-1 and SMP-2 have distinct functions, as well as localizations within the flagella and associated flagellar pocket. Third, loss of SMP-1 was associated with

alterations in the flagellum membrane dynamics and accumulation of membrane vesicles in the flagellar matrix. Although it is conceivable that the membrane vesicles originated in the cytosol, membrane vesicles were never observed in the lower sections of flagella that were contained within the flagellar pocket. Increased vesicle formation in the cytosol around the base of the flagellum was also not observed. Similar membrane vesicles are also absent from the truncated flagella of amastigote stages that lack detectable levels of SMP-1 (data not shown). We therefore favour the hypothesis that these vesicles result from the spontaneous involution of the flagellar membrane, in unsupported sections of the flagella that extend beyond the flagellar pocket. Fourth, loss of SMP-1 resulted in increased sensitivity of the promastigote flagellar membrane to perturbations in lipid composition. Specifically, inhibitors of sterol and sphingolipid biosynthesis, which lead to the accumulation of sterol precursors and depletion of de novo synthesized sphingolipids, respectively, induced flagellar retraction in the *smp-1/smp-2*$^{-/-}$ mutant under conditions that had little or no effect on flagellar length in wild-type parasites or mutant parasites complemented with SMP-1. As the flagellar membranes of *Leishmania* are predicted to be rich in sterols and sphingolipids, based on the resistance of SMP-1 to extraction in cold 1% Triton X-100 (Tull et al., 2004), these data suggest that SMP-1 stabilizes the flagellar membrane from perturbations in lipid composition.

How might SMP-1 stabilize the flagellar membrane? Our existing data suggest that SMP-1 forms a densely packed coat on the inner leaflet of the flagellar membrane. This is supported by estimates of SMP-1 copy number (Tull et al., 2004) and the finding that SMP-1 forms relatively stable oligomers in vivo. This protein coat could stabilize the flagellar membrane by preventing the formation of non-planar membrane structures and endovesicles. Biological membranes that are rich in DRM lipids appear to be susceptible to endovesicularization under certain conditions. For example, the DRM-rich plasma membrane of human red blood cells undergoes extensive endovesicularization during glucose starvation or following treatment with a range of amphiphiles (Hagerstrand et al., 2000; Murphy et al., 2007). Alternatively, the SMP-1 scaffold might modulate lipid recruitment and/or packing in the flagellar membrane. It is well established that clustering of lipids or polypeptides in model phospholipid- and cholesterol-containing membranes can induce large-scale phase transitions and the coexistence of liquid-ordered and liquid-disordered domains (Hammond et al., 2005). A number of acylated eukaryotic proteins appear to induce similar localized phase changes in biological membranes as a result of their capacity to oligomerize in vivo. These include the caveolins, the reticulons and the PHB-domain-containing proteins belonging to the reggie/flotillin family (Bauer and Pelkmans, 2006; Langhorst et al., 2007; Parton and Simons, 2007; Solis et al., 2007). Similarly, a SMP-1 coat would be expected to generate a high density of saturated short chain fatty acids in the inner leaflet of the flagellar membrane, and to promote the formation of condensed lipid domains in this membrane. Regardless of the precise mechanism of action, expression of SMP-1 in *Leishmania* might represent an adaptation to the fluctuating temperatures and nutrient availability in the different host environments, which would, in turn, impact the physical properties and lipid composition of the flagellar membrane.

Although SMP-1 is one of the first flagellar membrane proteins shown to have a direct role in flagellum biogenesis, an increasing number of non-flagellar proteins are thought to regulate protein and lipid trafficking to the flagellar membrane (Avidor-Reiss et al., 2004; Cuvillier et al., 2000; Dwyer et al., 2001; Hu et al., 2007; Nachury et al., 2007; Pullen et al., 2004; Qin et al., 2005; Rosenbaum and Witman, 2002; Sahin et al., 2008a; Scholey and Anderson, 2006; Wei et al., 2008). Several of these proteins have defined roles in regulating membrane trafficking between the Golgi complex, endosomes and the plasma membrane. For example, decreased expression of the phosphatidylinositol-(1,4)-phosphate adaptor protein-2 (FAPP-2) in Madin-Darby canine kidney cells impairs the outgrowth of primary cilia in these cells (Vieira et al., 2006). FAPP-2 is required for the apical transport of raft lipids, suggesting that the delivery of these lipids is important for ciliogenesis (Vieira et al., 2006). Similarly, loss of function of the μ1 subunit of the AP-1 clathrin adaptor complex in olfactory neurons prevents the delivery of membrane vesicles to the dendrite membrane and the formation of normal cilia (Dwyer et al., 2001). Defects in membrane transport in *Leishmania* can also produce profound alterations in flagellar morphology. *Leishmania* mutants lacking components of the AP-1 complex develop short, swollen flagella similar to those observed after treatment with ketoconazole (Vince et al., 2008). These mutants accumulate sterols in endocytic compartments and are hypersensitive to both sterol and sphingolipid biosynthetic inhibitors indicating a general perturbation of lipid homeostasis (Vince et al., 2008). Similarly, overexpression of a GTP-fixed form of the small myristoylated Arl3A protein in *L. amazonensis* induces defects in post-Golgi endosome trafficking and a dramatic shortening of the flagellum (Sahin et al., 2008a; Sahin et al., 2008b). Genetic deletion of a number of other *Leishmania* cytoplasmic proteins also results in retraction of the flagellum (Tammana et al., 2008; Thiel et al., 2008; Wiese, 2007), although the precise role of these proteins in membrane transport or signaling is unknown. Collectively, these studies support the notion that the delivery and retention of specific lipids and proteins in the flagellar membrane, by mechanisms that are independent of IFT, are essential for normal flagellum biogenesis.

SMP-1 is the prototypic member of a family of proteins that are expressed in all pathogenic trypanosomatid parasites (Ersfeld et al., 2005; Tull et al., 2004). Most members of this family are predicted to be myristoylated (and in some cases palmitoylated); however, some lack discernible acylation or other membrane-targeting motifs. Acylated and non-acylated SMP-like sequences also occur at the N-termini of another family of trypanosmatid proteins, termed the calpain-like proteins (CALPs) (Ersfeld et al., 2005). The CALPs are multidomain proteins that, similarly to the SMPs, are poorly characterized at the functional level. We show here that SMP-1 contains a distinctive β-sandwich jelly-roll fold that is probably conserved in all SMP/CALP family members (Ersfeld et al., 2005). The jelly-roll super-fold is found in a functionally diverse group of proteins, which include carbohydrate-binding proteins (lectins, glucanases), bacterial toxins and viral coat proteins (Williams and Westhead, 2002). Interestingly, several of these proteins have been shown to form non-covalent homodimers and homotrimers and to assemble into large macromolecular complexes in vivo (Chattopadhyay et al., 2007; Nandhagopal et al., 2002), similarly to the results reported here for SMP-1. The homo-oligomerization of some of these proteins, such as the glucocorticoid-induced TNF receptor ligand, is concentration dependent (Chattopadhyay et al., 2007; Nandhagopal et al., 2002). In this respect, it is notable that non-acylated SMP-1 exists primarily as a monomer in solution, suggesting that the oligomerization of SMP-1 observed in vivo reflects the high packing densities of this protein in the plane of the flagellar membrane (Chattopadhyay et al., 2007). *T. brucei* and

related trypanosomes express an additional family of flagellum-targeted myristoylated or palmitoylated proteins, termed the flagellar Ca^{2+}-binding proteins (FCaBPs) (Buchanan et al., 2005; Godsel and Engman, 1999; Maldonado et al., 1997; Wingard et al., 2008). These proteins are rich in α-helices, lack the β-sandwich jelly-roll fold and do not appear to homo-oligomerize in solution or in vivo. These data suggest significant differences in the way these two families of proteins function in the flagella of *Leishmania* and trypanosomes.

In contrast to SMP-1, epitope-tagged SMP-2 was localized to an apical structure in promastigotes, probably the flagellar pocket membrane. This structure was continuous with the flagellar membrane, but distinct from the flagellar basal body, based on the solubility of SMP-2::HA in cold 1% Triton X-100. The localization of SMP-2::HA to this membrane appears to be saturable, because SMP-2::HA could be detected on the cell body membrane when levels of expression were elevated (supplementary material Fig. S1). At present, nothing is known about the function of SMP-2. Complementation of the *smp-1/smp-2*$^{-/-}$ mutant with SMP-2 had no effect on the growth or flagellar phenotype of the mutant. It is possible that SMP-2 has a subtle role in either stabilizing the flagellar pocket membrane, and/or regulating membrane transport to and from this membrane. The flagellar pocket is the sole site of exocytic and endocytic traffic in these parasites, and it will be of interest to determine whether loss of SMP-2 has an effect on membrane dynamics in the amastigote stage, which is thought to have lower rates of endocytosis and exocytosis (McConville et al., 2002). Further work is also required to define the signals that target SMP-1 and SMP-2 to the flagellar and flagellar pocket membranes, respectively. Dual acylation (myristoylation/palmitoylation) of SMP-1 is essential for flagellar targeting, but might not be sufficient (Tull et al., 2004). For example, other dually acylated proteins in *Leishmania* are either targeted to intracellular organelles or the exoplasmic leaflet of the plasma membrane (Denny et al., 2000; Mills et al., 2007). However, truncated versions of these proteins containing the N-terminal acylation domain are targeted to the flagellum (Mills et al., 2007), suggesting that the flagellar membrane is the default pathway for dually acylated proteins. By contrast, monoacylated proteins, such as SMP-2, appear to be excluded from the flagellar membrane, although they can be targeted to distinct intracellular and plasma membrane domains. These data suggest that mono and dual acylation are important targeting signals, but that additional targeting information must reside within the polypeptide domain.

Materials and Methods

Cell culture

L. major (MHOM/SU/73/5ASKH) promastigotes were cultivated at 27°C in Schneider's *Drosophila* or SDM79 medium containing 10% heat-inactivated fetal bovine serum. For the isolation of amastigotes stages, BALB/c mice were subcutaneously infected with 5×10^6 stationary phase promastigotes, and amastigotes recovered from the lesions (Naderer et al., 2006). For drug treatment, rapidly dividing wild-type and mutant parasites were grown in medium containing either myriocin (1 μg/ml; Sigma) or ketoconazole (0.5 μg/ml; Sigma).

Chromosomal deletion of SMP-1 and SMP-2, generation of genetic rescue plasmids and HA-tagged chimeras

The *L. major smp-1/smp-2* mutant was generated by sequential replacement of a 2.8 kb *SMP* locus containing the *SMP-2* and *SMP-1* ORFs in tandem with bleomycin- and puromycin-resistant cassettes. The 5′ untranslated region of *SMP-2* was amplified by a polymerase chain reaction (PCR) using *L. major* genomic DNA as a template. The 5′ primer CGGATATCCCACACGTAACGGAGCTAC and 3′ primer CGGAATTCGACTTGACGCTGGTCGTG were used to amplify a 1.8 kb 5′UTR, which was then cloned into the *Eco*RV and *Eco*RI sites of pBluescript II SK vector (Stratagene). The 3′UTR of *SMP-1* was amplified using the 5′ primer CGGGATCCGCGGAAAACGAAATGAAG and 3′ primer CGTCTAGAGCACACAGGCATGAAGGTAC and the 2.0 kb amplicon ligated into the *Bam*HI and *Xba*I sites of the pBluescript vector containing the *SMP-2* 5′UTR. The bleomycin- and puromycin-resistant cassettes were obtained from pXG-BLEO and pXG-PAC, respectively, using the *Xho*I site, which was blunt ended by Klenow-polymerase after digestion, and the *Bam*HI site. The corresponding fragments were gel-purified and cloned between the 5′UTR and 3′UTR using *Sma*I and *Bam*HI sites of the pBluescript vector. All constructs were verified by diagnostic digests and DNA sequencing. Plasmid DNAs were linearized with *Eco*RV and *Xba*I digestion and DNA (5 μg) transfected into *L. major* promastigotes by electroporation. Double-resistant clones, lacking both chromosomal alleles of *SMP-1* and *SMP-2* (*ΔSMP-1/2::BLEO/ΔSMP-1/2::PAC*), are referred to as *smp-1/smp-2*. For plasmid-based expression of *SMP-1*, the ORF was PCR amplified using the 5′ primer CGGGATCCTATGGGCTGCGGTGCTTC and the 3′ primer TGCTCTAGATTACTTGTCCTTCTCCGCC, digested with *Bam*HI and *Xba*I and ligated into the *Bam*HI and *Xba*I sites of pX-NEO plasmid. Similarly, the ORF of *SMP-2* was amplified with 5′ primer CGGGATCCTATGGGCGGCTCCAAC and the 3′ primer TGCTCTAGATTAGTTCGCTACCGC, digested with *Bam*HI and *Xba*I and ligated into the *Bam*HI and *Xba*I sites of the pX-HYG plasmid.

For expression of HA(3x)-tagged chimeras, PCR amplicons of *SMP-1* and *SMP-2* ORFs were amplified from genomic DNA and cloned into *Sma*I and *Bam*HI sites of pX-HA(3x) (Mullin et al., 2001). For the GST-SMP-1 chimera, SMP-1 was amplified from genomic DNA using the primers CGGGATCCATGGGCTGCGGTGCTTCT and CCTGCTCGAGCTTGTCCTTCTCCGCCTG and cloned into the *Bam*HI and *Xho*I sites of pGEX-6P3 (GE Healthcare).

Antibody preparation and Immunoblotting

Antibodies to SMP-1 were obtained as previously described (Tull et al., 2004). Antibodies to SMP-2 were raised by immunization of New Zealand white rabbits with the peptide R^{38}IVKRKKGHQTWAFY^{50}(C) coupled to diphtheria toxoid (Mimotopes) in Freund's adjuvant (Sigma). Antibodies were purified by affinity chromatography on a peptide-sulfoLink agarose affinity column (Pierce) eluted into 0.1 M Tris-HCl, pH 8 with 0.1 M glycine pH 2.5. Antibodies were stored in 50% glycerol at –20°C. For western blotting, proteins were electrophoretically transferred to PVDF^{PSQ} membrane (Millipore) and blocked with 5% powdered skim milk in Tris-buffered saline (TBS) containing 0.2% Tween-20. For immunodetection of SMP-HA chimeras, proteins were transferred to nitrocellulose membrane (Advantec, MFS) and blocked with 5 % powdered skimmed milk in TBS containing 0.05% Tween-20. The blots were probed with rabbit anti-SMP-1 (total serum, 1:1000 dilution) and rabbit anti-SMP-2 (1:50 dilution) diluted in 5% powdered skimmed milk. Anti-rabbit horseradish peroxidase-conjugated secondary antibody was diluted 1:2500 in 1% powdered skimmed milk and detected using ECL western detection system.

Microscopy

For immunofluorescence microscopy, *L. major* parasites were fixed in 4% paraformaldehyde (0°C, 15 minutes), washed and resuspended with PBS, and immobilize on poly-L-lysine-coated coverslips. Cells were dehydrated with methanol (0°C, 5 minutes), washed with PBS, and incubated with 50 mM ammonium chloride (25°C, 10 minutes). Fixed cells were blocked with 1% BSA in PBS (25°C, 30 min) and probed with anti-HA (Roche, 1:80 dilution), anti-tubulin (Sigma, 1:500 dilution) or SMP-1 antiserum (1:400 dilution). Secondary antibodies Alexa Fluor 488 goat anti-rat (1:200 dilution), Alexa Fluor 594 goat anti-mouse (1:1000 dilution) and Alexa Fluor 488/594 goat anti-rabbit (1:1000 dilution) were used. All antibodies were diluted in 1% BSA in PBS. Coverslips were mounted in Mowiol 4-88 (Calbiochem, La Jolla, CA) containing Hoechst 33342 (5 μg/ml, Molecular Probes). Cells were viewed at room temperature with a Zeiss Axioplan2 microscope (Thornwood, NY) using ×100 objective (1.3 numerical aperture) equipped with an AxioCamMrm digital camera, analysed with Axio Vision 4.5 (Zeiss) and assembled with Photoshop Elements v6 (Adobe Systems).

For video microscopy, a drop of promastigote culture was placed onto a slide and covered gently with a coverslip. The whole mount was sealed with VALAP (equal parts paraffin wax:lanolin:vaseline, melted at about 40°C). Samples were examined with a Leica DMRB microscope using either Phase or differential interference contrast (DIC) optics, usually using a ×20 or ×40 objective. Images were viewed with a Panasonic F250 CCD PAL colour video camera and recorded in real time using Panasonic AU-550 tape deck on to metal MII tapes. Quantitative measurements were undertaken using Image I (Universal Imaging) software.

For SEM, log-phase promastigotes were washed in PBS followed by fixation for one hour with 2.5% glutaraldehyde (ProSciTech) in PBS. Cells were washed three times in PBS followed with a drop of cell suspension then placed onto a circular 1% polyethylenimine (Sigma)-coated coverslip for several minutes. Affixed cells were rinsed in distilled H_2O and slowly dehydrated in a graded series of ethanol. Samples in 100% ethanol were then critical-point dried using a Baltec CPD 030 and gold coated with an Edwards S150B sputter coater and observed at 20 KV with a Philips XL30 FEG Field Emission Scanning Electron Microscope.

A semi-simultaneous fixation protocol (Tippit and Pickett-Heaps, 1977) was used to prepare parasites for transmission electron microscopy (TEM). Briefly, promastigotes were washed in PBS followed by fixation for 5-10 seconds with 0.5% glutaraldehyde (ProSciTech) in PBS. An equal volume of 1% OsO_4 in PBS was added after 10 seconds and the mixture was incubated for 20 minutes. Samples were washed three times in distilled H_2O then stained overnight at 4°C with 2% aqueous uranyl

acetate (ProSciTech), followed by slow dehydration in a graded ethanol series and a final three exchanges of 100% ethanol. Following dehydration, samples were infiltrated with increasing concentrations of Spurr's resin up to 100%. Following three changes of 100% resin the samples were polymerised overnight at 70°C. Sections (90 nm) were cut using a Leica Ultracut R ultramicrotome (Leica Microsystems) and Diatome diamond knife for collection onto 200 mesh copper grids (ProSciTech). Sections were post-stained with 2% uranyl acetate for 10 minutes, washed three times in distilled H_2O then stained using a triple-lead solution for 5 minutes. Samples were examined using a Philips BioTwin CM 120 transmission electron microscope (Philips) and images taken with a Gatan 791 Multiscan camera.

NMR analysis of SMP-1

A GST-SMP-1 fusion protein was labeled with ^{15}N- and ^{13}C-labeled SMP-1 (Marley et al., 2001) and purified on glutathione-Sepharose. The GST portion was cleaved with Precision Protease (Pharmacia) and the free GST removed by passage over glutathione-Sepharose. All NMR data sets were acquired at 25°C on a Varian Inova 600 MHz spectrometer. The solution conditions were 50 mM phosphate, pH 6.8, 5 mM DTT and where appropriate 10% ^2H_2O and 90% H_2O or 100% ^2H_2O. Expression and purification of SMP-1 and the assignment of the ^1H, ^{13}C and ^{15}N resonances of SMP-1 are published elsewhere (Gooley et al., 2006). Distance structural constraints were obtained from 3D ^{15}N-edited NOESY-HSQC, ^{13}C-edited HSQC-NOESY and ^{13}C(aromatic)-edited HSQC-NOESY (all with mixing times of 100 mseconds) spectra. A limited number of χ_1 angles were obtained from inspection of 3D HNHB, HACAHB, 2D ^{15}N-{$^{13}C\gamma$} or $^{13}C'$-{$^{13}C\gamma$} spin-echo difference ^1H{^{15}N}-HSQC experiments (Hu and Bax, 1997). For the stereospecific assignment of methyl residues of Val and Leu residues a ^{13}C-constant time HSQC experiment was acquired on a sample expressed from medium containing 10% [^{13}C]glucose and 90% [^{12}C]glucose (Neri et al., 1989). A total of ten Val (out of 12) and six Leu (out of seven) were stereospecifically assigned. All NMR data sets were processed in NMRPipe (Delaglio et al., 1995) and analysed in NMRView (Johnson, 2004).

NOE data were assigned using the CANDID module of CYANA (version 1.0.7) with rounds of both manual and automatic assignment (Herrmann et al., 2002). Backbone ϕ,ψ dihedral angle constraint data was generated from TALOS (Cornilescu et al., 1999) and these data complemented with χ_1 constraint data qualitatively determined from inspecting the relevant spectra (supplementary material Table S1). The NOE constraints were further added to and refined with calculations using XPLOR-NIH (version 2.9.7) using a simulated annealing protocol with dynamics in both torsion and cartesian space (Schwieters et al., 2003). The final force constants used were: 50 kcal mol^{-1} for experimental distance constraints, 200 kcal mol^{-1} rad^{-2} for dihedral angle constraints, and 1.0 kcal mol^{-1} for the Ramachandran database potential of mean force (Kuszewski et al., 1996; Mertens and Gooley, 2005). Structures were validated in PROCHECK-NMR (Laskowski et al., 1996) and inspected in MOLMOL (Koradi et al., 1996) and PyMOL (http://www.pymol.org). Structural similarity was accessed using DALI (Holm and Sander, 1996). The coordinates and NMR restraints have been deposited with the PDB code 2FE0.

Cross-linking SMP-1 protein oligomers

L. major promastigotes (2×10^7) were harvested by centrifugation (2000 ***g***, 25°C, 10 minutes), washed with PBS, and extracted with 200 µl 1% Triton X-100 at 0°C for 30 minutes. Detergent-resistant membranes and cytoskeletal components were recovered by centrifugation, and resuspended in PBS (50 µl) containing DTSSP in PBS (2 µl, 55 mM, Pierce) and incubated with gentle mixing at 4°C for 2 hours. Excess DTSSP was quenched by addition of Tris-HCl, pH 7.4 buffer (3 µl, 1 M) and incubation at room temperature for 30 minutes. Proteins were extracted in non-reducing SDS sample buffer, separated in a 15% SDS PAGE gel and electrophoretically transferred to $PVDF^{PSQ}$ membrane for immunoblot analysis as described above.

L. major promastigotes (6×10^7) were harvested by centrifugation (2000 ***g***, 25°C, 10 minutes) and washed with PBS. Live cells were resuspended in 50 µl PBS, containing DSS (4 µl, 54 mM in DMSO, Pierce) and incubated at room temperature for 2 hours. Excess DSS was quenched by addition of Tris-HCl, pH 7.4 buffer (16 µl, 1 M) and incubation at room temperature for 60 minutes. Cells were extracted with 1% Triton-X 100 at 0°C for 30 min, centrifuged (10,000 ***g***, 10 minutes, 0°C), and proteins in the supernatant and pellet fractions analysed by 12% SDS-PAGE and immunoblotting as described above.

2D-BN-SDS PAGE

L. major promastigotes (6×10^7) were harvested by centrifugation, washed twice with PBS, and extracted with 0.5% lauryl maltoside buffer containing 20 mM Tris-HCl, pH 7.4, 50 mM NaCl, 10% glycerol, 0.1 mM EDTA and Complete protease inhibitor cocktail (Roche) (220 µl, 0°C, 10 minutes). Insoluble material was removed by centrifugation, and the supernatant diluted with sample loading buffer (50 µl containing 5% Coomassie Blue G and 500 mM amino caproic acid in 100 mM Bis-Tris, pH 7). Protein complexes in the mixture were resolved on a 5-12% large format BN-PAGE gel using an anode buffer containing 50 mM Bis-Tris pH7 and a blue cathode buffer containing 0.02% Brilliant Blue, 50 mM Tricine and 15 mM Bis-Tris, pH 7 (Schamel, 2008). The blue cathode buffer was exchanged for clear cathode buffer (50 mM Tricine and 15 mM Bis-Tris, pH 7) when the dye front was a quarter of the way through the resolving gel. BN-PAGE gel lanes were either stained with Coomassie or incubated in a solution of 20 mM DTT and SDS running buffer for 20 minutes. Proteins in the complexes were resolved in a second dimension on a 15% SDS-PAGE gel and electrophoretically transferred to $PVDF^{PSQ}$ membrane for immunoblot analysis as described above.

This work was funded by an Australian NH&MRC Program grant. M.J.M. is a NH&MRC Principal Research Fellow. G.I.M. is an ARC Federation Fellow. We dedicate this paper to Tim Spurck, a highly valued colleague and friend.

Supplementary material available online at
http://jcs.biologists.org/cgi/content/full/123/4/544/DC1

References

Absalon, S., Blisnick, T., Kohl, L., Toutirais, G., Dore, G., Julkowska, D., Tavenet, A. and Bastin, P. (2008). intraflagellar transport and functional analysis of genes required for Flagellum formation in Trypanosomes. *Mol. Biol. Cell* **19**, 929-944.

Arakaki, T., Le Trong, I., Phizicky, E., Quartley, E., DeTitta, G., Luft, J., Lauricella, A., Anderson, L., Kalyuzhniy, O., Worthey, E. et al. (2003). A structure of Lmaj006129AAA, a hypothetical protein from Leishmania major. *Acta Crystallogr. Sect. F Struct. Biol. Cryst. Commun.* **62**, 175-179.

Avidor-Reiss, T., Maer, A. M., Koundakjian, E., Polyanovsky, A., Keil, T., Subramaniam, S. and Zuker, C. S. (2004). Decoding cilia function: defining specialized genes required for compartmentalized cilia biogenesis. *Cell* **117**, 527-539.

Bae, Y. K., Qin, H., Knobel, K. M., Hu, J., Rosenbaum, J. L. and Barr, M. M. (2006). General and cell-type specific mechanisms target TRPP2/PKD-2 to cilia. *Development* **133**, 3859-3870.

Bauer, M. and Pelkmans, L. (2006). A new paradigm for membrane-organizing and -shaping scaffolds. *FEBS Lett.* **580**, 5559-5564.

Bonhivers, M., Nowacki, S., Landrein, N. and Robinson, D. R. (2008). Biogenesis of the trypanosome endo-exocytotic organelle is cytoskeleton mediated. *PLoS Biol.* **6**, e105.

Broadhead, R., Dawe, H. R., Farr, H., Griffiths, S., Hart, S. R., Portman, N., Shaw, M. K., Ginger, M. L., Gaskell, S. J., McKean, P. G. et al. (2006). Flagellar motility is required for the viability of the bloodstream trypanosome. *Nature* **440**, 224-227.

Buchanan, K. T., Ames, J. B., Asfaw, S. H., Wingard, J. N., Olson, C. L., Campana, P. T., Araujo, A. P. and Engman, D. M. (2005). A flagellum-specific calcium sensor. *J. Biol. Chem.* **280**, 40104-40111.

Chattopadhyay, K., Ramagopal, U. A., Mukhopadhaya, A., Malashkevich, V. N., Dilorenzo, T. P., Brenowitz, M., Nathenson, S. G. and Almo, S. C. (2007). Assembly and structural properties of glucocorticoid-induced TNF receptor ligand: Implications for function. *Proc. Natl. Acad. Sci. USA* **104**, 19452-19457.

Cornilescu, G., Delaglio, F. and Bax, A. (1999). Protein backbone angle restraints from searching a database for chemical shift and sequence homology. *J. Biomol. NMR* **13**, 289-302.

Cuvillier, A., Redon, F., Antoine, J. C., Chardin, P., DeVos, T. and Merlin, G. (2000). LdARL-3A, a Leishmania promastigote-specific ADP-ribosylation factor-like protein, is essential for flagellum integrity. *J. Cell Sci.* **113**, 2065-2074.

Davidge, J. A., Chambers, E., Dickinson, H. A., Towers, K., Ginger, M. L., McKean, P. G. and Gull, K. (2006). Trypanosome IFT mutants provide insight into the motor location for mobility of the flagella connector and flagellar membrane formation. *J. Cell Sci.* **119**, 3935-3943.

Delaglio, F., Grzesiek, S., Vuister, G. W., Zhu, G., Pfeifer, J. and Bax, A. (1995). NMRPipe: a multidimensional spectral processing system based on UNIX pipes. *J. Biomol. NMR* **6**, 277-293.

Denny, P. W., Gokool, S., Russell, D. G., Field, M. C. and Smith, D. F. (2000). Acylation-dependent protein export in Leishmania. *J. Biol. Chem.* **275**, 11017-11025.

Denny, P. W., Goulding, D., Ferguson, M. A. and Smith, D. F. (2004). Sphingolipid-free Leishmania are defective in membrane trafficking, differentiation and infectivity. *Mol. Microbiol.* **52**, 313-327.

Dwyer, N. D., Adler, C. E., Crump, J. G., L'Etoile, N. D. and Bargmann, C. I. (2001). Polarized dendritic transport and the AP-1 mu1 clathrin adaptor UNC-101 localize odorant receptors to olfactory cilia. *Neuron.* **31**, 277-287.

Ersfeld, K., Barraclough, H. and Gull, K. (2005). Evolutionary relationships and protein domain architecture in an expanded calpain superfamily in kinetoplastid parasites. *J. Mol. Evol.* **61**, 742-757.

Ginger, M. L., Portman, N. and McKean, P. G. (2008). Swimming with protists: perception, motility and flagellum assembly. *Nat. Rev. Microbiol.* **6**, 838-850.

Godsel, L. M. and Engman, D. M. (1999). Flagellar protein localization mediated by a calcium-myristoyl/palmitoyl switch mechanism. *EMBO J.* **18**, 2057-2065.

Gooley, P. R., Mertens, H. D., Tull, D. and McConville, M. J. (2006). 1H, 13C and 15N resonance assignments of SMP-1: a small myristoylated protein from Leishmania major. *J. Biomol. NMR* **36**, 26.

Hagerstrand, H., Danieluk, M., Bobrowska-Hagerstrand, M., Iglic, A., Wrobel, A., Isomaa, B. and Nikinmaa, M. (2000). Influence of band 3 protein absence and skeletal structures on amphiphile- and Ca(2+)-induced shape alterations in erythrocytes: a study with lamprey (Lampetra fluviatilis), trout (Onchorhynchus mykiss) and human erythrocytes. *Biochim. Biophys. Acta* **1466**, 125-138.

Hammond, A. T., Heberle, F. A., Baumgart, T., Holowka, D., Baird, B. and Feigenson, G. W. (2005). Crosslinking a lipid raft component triggers liquid ordered-liquid disordered phase separation in model plasma membranes. *Proc. Natl. Acad. Sci. USA* **102**, 6320-6325.

Herrmann, T., Guntert, P. and Wuthrich, K. (2002). Protein NMR structure determination with automated NOE-identification in the NOESY spectra using the new software ATNOS. *J. Biomol. NMR* **24**, 171-189.

Hertz-Fowler, C., Ersfeld, K. and Gull, K. (2001). CAP5.5, a life-cycle-regulated, cytoskeleton-associated protein is a member of a novel family of calpain-related proteins in Trypanosoma brucei. *Mol. Biochem. Parasitol.* **116**, 25-34.

Holm, L. and Sander, C. (1996). Mapping the protein universe. *Science* **273**, 595-603.

Hu, J., Wittekind, S. G. and Barr, M. M. (2007). STAM and Hrs down-regulate ciliary TRP receptors. *Mol. Biol. Cell* **18**, 3277-3289.

Hu, J. S. and Bax, A. (1997). Chi 1 angle information from a simple two-dimensional NMR experiment that identifies trans 3JNC gamma couplings in isotopically enriched proteins. *J. Biomol. NMR* **9**, 323-328.

Johnson, B. A. (2004). Using NMRView to visualize and analyze the NMR spectra of macromolecules. *Methods Mol. Biol.* **278**, 313-352.

Kohl, L., Robinson, D. and Bastin, P. (2003). Novel roles for the flagellum in cell morphogenesis and cytokinesis of trypanosomes. *EMBO J.* **22**, 5336-5346.

Koradi, R., Billeter, M. and Wuthrich, K. (1996). MOLMOL: a program for display and analysis of macromolecular structures. *J. Mol. Graph* **14**, 51-55, 29-32.

Kuszewski, J., Gronenborn, A. M. and Clore, G. M. (1996). Improving the quality of NMR and crystallographic protein structures by means of a conformational database potential derived from structure databases. *Protein Sci.* **5**, 1067-1080.

Langhorst, M. F., Solis, G. P., Hannbeck, S., Plattner, H. and Stuermer, C. A. (2007). Linking membrane microdomains to the cytoskeleton: regulation of the lateral mobility of reggie-1/flotillin-2 by interaction with actin. *FEBS Lett.* **581**, 4697-4703.

Laskowski, R. A., Rullmannn, J. A., MacArthur, M. W., Kaptein, R. and Thornton, J. M. (1996). AQUA and PROCHECK-NMR: programs for checking the quality of protein structures solved by NMR. *J. Biomol. NMR* **8**, 477-486.

Maldonado, R. A., Linss, J., Thomaz, N., Olson, C. L., Engman, D. M. and Goldenberg, S. (1997). Homologues of the 24-kDa flagellar Ca(2+)-binding protein gene of Trypanosoma cruzi are present in other members of the Trypanosomatidae family. *Exp. Parasitol.* **86**, 200-205.

Marley, J., Lu, M. and Bracken, C. (2001). A method for efficient isotopic labeling of recombinant proteins. *J. Biomol. NMR* **20**, 71-75.

McConville, M. J., Mullin, K. A., Ilgoutz, S. C. and Teasdale, R. D. (2002). Secretory pathway of trypanosomatid parasites. *Microbiol. Mol. Biol. Rev.* **66**, 122-154.

Mertens, H. D. and Gooley, P. R. (2005). Validating the use of database potentials in protein structure determination by NMR. *FEBS Lett.* **579**, 5542-5548.

Mills, E., Price, H. P., Johner, A., Emerson, J. E. and Smith, D. F. (2007). Kinetoplastid PPEF phosphatases: dual acylated proteins expressed in the endomembrane system of Leishmania. *Mol. Biochem. Parasitol.* **152**, 22-34.

Mullin, K. A., Foth, B. J., Ilgoutz, S. C., Callaghan, J. M., Zawadzki, J. L., McFadden, G. I. and McConville, M. J. (2001). Regulated degradation of an endoplasmic reticulum membrane protein in a tubular lysosome in Leishmania mexicana. *Mol. Biol. Cell* **12**, 2364-2377.

Murphy, S. C., Fernandez-Pol, S., Chung, P. H., Prasanna Murthy, S. N., Milne, S. B., Salomao, M., Brown, H. A., Lomasney, J. W., Mohandas, N. and Haldar, K. (2007). Cytoplasmic remodeling of erythrocyte raft lipids during infection by the human malaria parasite Plasmodium falciparum. *Blood* **110**, 2132-2139.

Nachury, M. V., Loktev, A. V., Zhang, Q., Westlake, C. J., Peranen, J., Merdes, A., Slusarski, D. C., Scheller, R. H., Bazan, J. F., Sheffield, V. C. et al. (2007). A core complex of BBS proteins cooperates with the GTPase Rab8 to promote ciliary membrane biogenesis. *Cell* **129**, 1201-1213.

Naderer, T., Ellis, M. A., Sernee, M. F., De Souza, D. P., Curtis, J., Handman, E. and McConville, M. J. (2006). Virulence of Leishmania major in macrophages and mice requires the gluconeogenic enzyme fructose-1,6-bisphosphatase. *Proc. Natl. Acad. Sci. USA* **103**, 5502-5507.

Nandhagopal, N., Simpson, A. A., Gurnon, J. R., Yan, X., Baker, T. S., Graves, M. V., Van Etten, J. L. and Rossmann, M. G. (2002). The structure and evolution of the major capsid protein of a large, lipid-containing DNA virus. *Proc. Natl. Acad. Sci. USA* **99**, 14758-14763.

Neri, D., Szyperski, T., Otting, G., Senn, H. and Wuthrich, K. (1989). Stereospecific nuclear magnetic resonance assignments of the methyl groups of valine and leucine in the DNA-binding domain of the 434 repressor by biosynthetically directed fractional 13C labeling. *Biochemistry* **28**, 7510-7516.

Oberholzer, M., Bregy, P., Marti, G., Minca, M., Peier, M. and Seebeck, T. (2007). Trypanosomes and mammalian sperm: one of a kind? *Trends Parasitol.* **23**, 71-77.

Parton, R. G. and Simons, K. (2007). The multiple faces of caveolae. *Nat. Rev. Mol. Cell. Biol.* **8**, 185-194.

Pullen, T. J., Ginger, M. L., Gaskell, S. J. and Gull, K. (2004). Protein targeting of an unusual, evolutionarily conserved adenylate kinase to a eukaryotic flagellum. *Mol. Biol. Cell* **15**, 3257-3265.

Qin, H., Burnette, D. T., Bae, Y. K., Forscher, P., Barr, M. M. and Rosenbaum, J. L. (2005). Intraflagellar transport is required for the vectorial movement of TRPV channels in the ciliary membrane. *Curr. Biol.* **15**, 1695-1699.

Ralston, K. S. and Hill, K. L. (2008). The flagellum of Trypanosoma brucei: new tricks from an old dog. *Int. J. Parasitol.* **38**, 869-884.

Ralton, J. E., Mullin, K. A. and McConville, M. J. (2002). Intracellular trafficking of glycosylphosphatidylinositol (GPI)-anchored proteins and free GPIs in Leishmania mexicana. *Biochem. J.* **363**, 365-375.

Rosenbaum, J. L. and Witman, G. B. (2002). Intraflagellar transport. *Nat. Rev. Mol. Cell. Biol.* **3**, 813-825.

Sahin, A., Espiau, B., Marchand, C. and Merlin, G. (2008a). Flagellar length depends on LdARL-3A GTP/GDP unaltered cycling in Leishmania amazonensis. *Mol. Biochem. Parasitol.* **157**, 83-87.

Sahin, A., Espiau, B., Tetaud, E., Cuvillier, A., Lartigue, L., Ambit, A., Robinson, D. R. and Merlin, G. (2008b). The leishmania arl-1 and Golgi traffic. *PLoS ONE* **3**, e1620.

Schamel, W. W. (2008). Two-dimensional blue native polyacrylamide gel electrophoresis. *Curr. Protoc. Cell Biol.* **Chapter 6**, Unit 6, p. 10.

Scholey, J. M. and Anderson, K. V. (2006). Intraflagellar transport and cilium-based signaling. *Cell* **125**, 439-442.

Schwieters, C. D., Kuszewski, J. J., Tjandra, N. and Clore, G. M. (2003). The Xplor-NIH NMR molecular structure determination package. *J. Magn. Reson.* **160**, 65-73.

Solis, G. P., Hoegg, M., Munderloh, C., Schrock, Y., Malaga-Trillo, E., Rivera-Milla, E. and Stuermer, C. A. (2007). Reggie/flotillin proteins are organized into stable tetramers in membrane microdomains. *Biochem. J.* **403**, 313-322.

Tammana, T. V. S., Sahasrabuddhe, A. A., Mitra, K., Bajpai, V. K. and Gupta, C. M. (2008). Actin depoylmerizing factor, ADF/cofilin, is essentially required in assembly of Leishmania flagelum. *Mol. Microbiol.* **70**, 837-852.

Thiel, M., Harder, S., Wiese, M., Kroemer, M. and Bruchhaus, I. (2008). Involvement of a Leishmania thymidine kinase in flagellum formation, promastigote shape and growth as well as virulence. *Mol. Biochem. Parasitol.* **158**, 152-162.

Tippit, D. H. and Pickett-Heaps, J. D. (1977). Mitosis in the pennate diatom *Surirella ovalis*. *J. Cell Biol*. **73**, 705-727.

Tull, D., Vince, J. E., Callaghan, J. M., Naderer, T., Spurck, T., McFadden, G. I., Currie, G., Ferguson, K., Bacic, A. and McConville, M. J. (2004). SMP-1, a member of a new family of small myristoylated proteins in kinetoplastid parasites, is targeted to the flagellar membrane in Leishmania. *Mol. Biol. Cell* **15**, 4775-4786.

Vieira, O. V., Gaus, K., Verkade, P., Fullekrug, J., Vaz, W. L. and Simons, K. (2006). FAPP2, cilium formation, and compartmentalization of the apical membrane in polarized Madin-Darby canine kidney (MDCK) cells. *Proc. Natl. Acad. Sci. USA* **103**, 18556-18561.

Vince, J. E., Tull, D. L., Spurck, T., Derby, M. C., McFadden, G. I., Gleeson, P. A., Gokool, S. and McConville, M. J. (2008). Leishmania adaptor protein-1 subunits are required for normal lysosome traffic, flagellum biogenesis, lipid homeostasis, and adaptation to temperatures encountered in the mammalian host. *Eukaryot. Cell* **7**, 1256-1267.

Wei, H. C., Rollins, J., Fabian, L., Hayes, M., Polevoy, G., Bazinet, C. and Brill, J. A. (2008). Depletion of plasma membrane PtdIns(4,5)P2 reveals essential roles for phosphoinositides in flagellar biogenesis. *J. Cell Sci.* **121**, 1076-1084.

Wiese, M. (2007). Leishmania MAP kinases-familiar proteins in an unusual context. *Int. J. Parasitol.* **37**, 1053-1062.

Williams, A. and Westhead, D. R. (2002). Sequence relationships in the legume lectin fold and other jelly rolls. *Protein Eng.* **15**, 771-774.

Wingard, J. N., Ladner, J., Vanarotti, M., Fisher, A. J., Robinson, H., Buchanan, K. T., Engman, D. M. and Ames, J. B. (2008). Structural insights into membrane targeting by the flagellar calcium-binding protein (FCaBP), a myristoylated and palmitoylated calcium sensor in Trypanosoma cruzi. *J. Biol. Chem.* **283**, 23388-23396.

Zhang, K., Showalter, M., Revollo, J., Hsu, F. F., Turk, J. and Beverley, S. M. (2003). Sphingolipids are essential for differentiation but not growth in Leishmania. *EMBO J.* **22**, 6016-6026.

Zuo, X., Guo, W. and Lipschutz, J. H. (2009). The exocyst protein Sec10 is necessary for primary ciliogenesis and cystogenesis in vitro. *Mol. Biol. Cell* **20**, 2522-2529.